EPJ Web of Conferences **63**, 02021 (2013)
DOI: 10.1051/epjconf/ 20136302021

Clusters, Halos, And S-Factors In Fermionic Molecular Dynamics ⋆

Hans Feldmeier[1] and Thomas Neff[1]

[1] *GSI Helmholtzzentrum für Schwerionenforschung GmbH, Darmstadt*

Abstract. In Fermionic Molecular Dynamics antisymmetrized products of Gaussian wave packets are projected on angular momentum, linear momentum, and parity. An appropriately chosen set of these states span the many-body Hilbert space in which the Hamiltonian is diagonalized. The wave packet parameters – position, momentum, width and spin – are obtained by variation under constraints. The great flexibility of this basis allows to describe not only shell-model like states but also exotic states like halos, e.g. the two-proton halo in ^{17}Ne, or cluster states as they appear for example in ^{12}C close to the α breakup threshold where the Hoyle state is located. Even a fully microscopic calculation of the ^{3}He(α,γ)^{7}Be capture reaction is possible and yields an astrophysical S-factor that compares very well with newer data. As representatives of numerous results these cases will be discussed in this contribution, some of them not published so far. The Hamiltonian is based on the realistic Argonne V18 nucleon-nucleon interaction.

1 Fermionic Molecular Dynamics (FMD)

In the FMD approach we employ Gaussian wave packets

$$\langle \mathbf{x}|q\rangle = \exp\left\{-\frac{(\mathbf{x}-\mathbf{b})^2}{2a}\right\} \otimes \left|\chi^{\uparrow},\chi^{\downarrow}\right\rangle \otimes \left|\xi\right\rangle \qquad (1)$$

as single-particle basis states. The complex parameters **b** encode the mean positions and momenta of the wave packets and a the widths of the wave packets. The spins can assume any direction, isospin is ± 1 denoting a proton or a neutron. Intrinsic many-body basis states are Slater determinants

$$\left|Q\right\rangle = \mathcal{A}\left\{\left|q_1\right\rangle \otimes \ldots \otimes \left|q_A\right\rangle\right\} \qquad (2)$$

that reflect deformation or clustering and break the symmetries of the Hamiltonian with respect to parity, rotation and translation. To restore the symmetries the intrinsic basis states are projected on parity, angular momentum and total linear momentum

$$\left|Q; J^{\pi}MK; \mathbf{P}=0\right\rangle = \hat{P}^{\pi}\hat{P}^{J}_{MK}\hat{P}^{\mathbf{P}=0}\left|Q\right\rangle. \qquad (3)$$

In a full FMD calculation the many-body Hilbert space is spanned by a set of N projected intrinsic basis states $\left\{\left|Q^{(a)}; J^{\pi}MK; \mathbf{P}=0\right\rangle, a=1,\ldots,N\right\}$. By diagonalizing the Hamiltonian in this set of non-orthogonal basis states the amplitudes of the various configurations contained in the many-body eigenstate are determined.

Starting from the realistic Argonne V18 interaction [1] we derive a phase-shift-equivalent effective low-momentum interaction using the unitary correlation operator method (UCOM). The basic idea of the UCOM approach is to explicitly include short-range central and tensor correlations by means of a unitary operator [2–4]. No-core shell model calculations show that the two-body UCOM interaction gives a good description of s- and light p-shell nuclei [4], indicating that the neglected induced 3-body forces cancel to a certain extent the missing genuine 3-body forces.

2 Cluster States in ^{12}C

The structure of the second 0^+_2 state in ^{12}C, the Hoyle state, is enjoying renewed and still growing interest in nuclear structure research [5–9]. In [10] we investigated its structure with a model space spanned by angular momentum projected FMD configurations obtained by variation plus a full set of projected three-α triangular configurations. We found that the Hoyle state is very dilute and extended, consisting mainly of well distinguished α-clusters. This is illustrated in the top part of Fig. 1 where we show the density distribution of those intrinsic FMD basis states that have the largest overlap with the ground state and the Hoyle state.

While the leading intrinsic configuration of the ground state is very compact, and after projection on good angular momentum, essentially a shell model state filling the $p_{3/2}$-shell, the Hoyle state is a quantal superposition of three α-clusters arranged in a slightly opened triangle configuration, or one may regard it also as a ^{8}Be surrounded by an α-cluster, see upper part of Fig. 1.

The first 2^+ state has the same leading intrinsic configuration as the ground state and may thus be regarded as the $J^{\pi} = 2^+$ member of a rotational band based on the ground state. The analogue argument does not hold for the second 2^+ state, it does not quite look like the 2^+ member of a rotational band with the same intrinsic structure as the

⋆ Supported by the ExtreMe Matter Institute EMMI

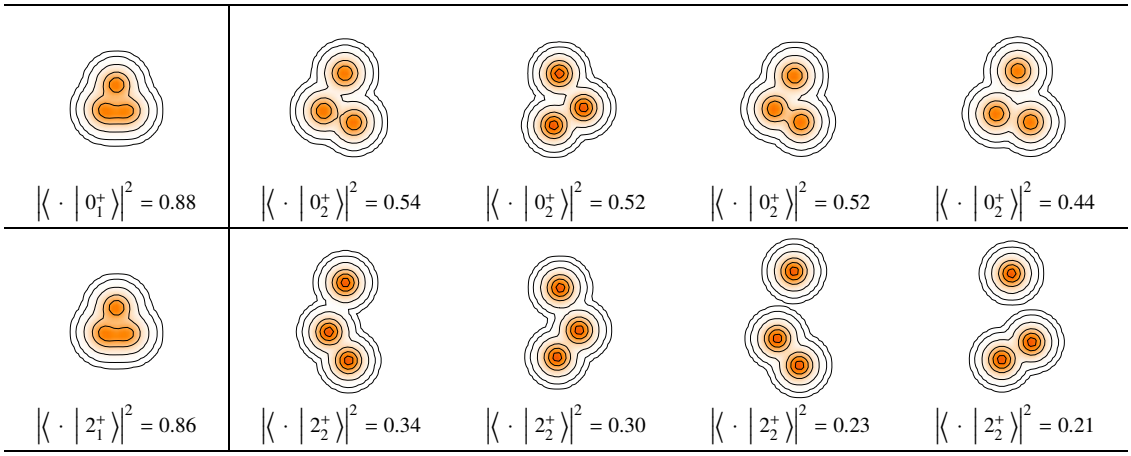

Figure 1. Top: density of intrinsic FMD basis states that have the largest overlaps with the ground (0_1^+) and Hoyle (0_2^+) state, respectively. Note that FMD states are not orthogonal. Bottom: same as top, but for the for 2_1^+ and 2_2^+ states. The 0_1^+ and the 0_2^+ states have different intrinsic structures and thus the recently identified 0_2^+ is not just simply a rotating Hoyle state.

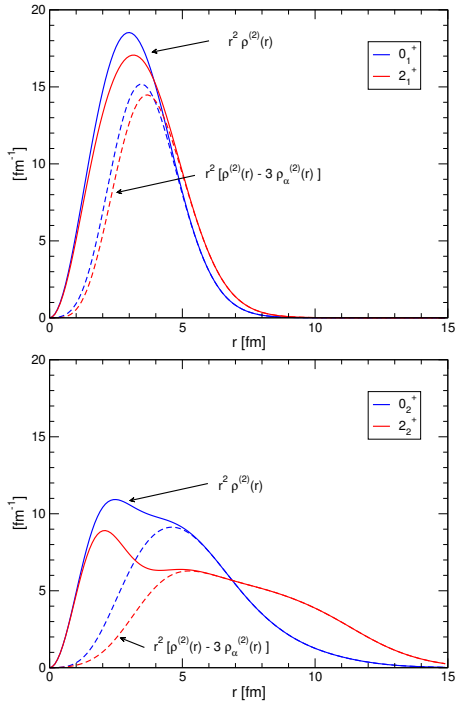

Figure 2. Top: full lines denote two-body densities as function of distance r between particle pairs of ^{12}C ground state rotational band members 0_1^+(blue) and 2_1^+ state (red); dashed lines show result when the distribution of pairs where both particles are inside the same α-cluster are subtracted [9]. This indicates distance distributions of pairs, where the two particles are in different α-clusters. Bottom: same as top, but for the Hoyle state "rotational band" members 0_2^+(blue) and 2_2^+ state (red). See also Fig. 1.

Hoyle state (lower part of Fig. 1). There is still the ^{8}Be correlation but the third α-cluster is pushed further away by centrifugal forces and feels attraction to only one of the ^{8}Be α-clusters, thus forming obtuse triangles.

Although intrinsic FMD basis states provide an intuitive understanding of the structure of the many-body state, they are not observable. Therefore we proposed in Ref. [9] to look at the two-body density

$$\rho^{(2)}(\mathbf{r}) = \langle \Psi \Big| \sum_{i<j} \delta(\hat{\mathbf{r}}_i - \hat{\mathbf{r}}_j - \mathbf{r}) \Big| \Psi \rangle \,, \qquad (4)$$

which gives the probability to find a pair of nucleons at a distance $\mathbf{r}$. This correlation function can be calculated in any representation and can thus be used to compare different many-body approaches.

Fig. 2 shows that in the 2_1^+ state the distances between nucleons are slightly larger than in the ground state but otherwise very similar. The lower part of Fig. 2 reveals much larger particle distances for the 0_2^+ (Hoyle) and the 2_2^+ state. In the Hoyle state a shoulder appears around 5 fm indicating the pairs where one particle is in one α-cluster and the other one in the neighbouring α-cluster, compare Fig. 1 (5 fm is the typical distance between the centers of the clusters). The maximum around 2 fm originates from pairs within the same cluster. The picture becomes even more transparent when we subtract three times the pair distributions of a single α-cluster (dashed lines). The distribution of the dilute Hoyle-like 2_2^+ state shows a broad shoulder between 5 and 10 fm coming from pairs with one nucleon in the distant α-cluster and one in the ^{8}Be-like structure, see lower part of Fig. 1.

Both, the recently measured energy of the 2_2^+ resonance and its $B(E2)$-value of the transition to the ground state [6] compare well with our predictions, see Table 1.

We used these many-body wave functions also to calculate the transition form factor from the ground state to the Hoyle state and compared it directly to electron scattering data [10, 11]. Our results are similar to those of [12, 13] where a many-body state representing a gas of independent α-clusters is assumed. The good agreement between calculated and measured form factors is a strong confirmation for a spatially extended cluster structure of the Hoyle state. The overall agreement with many other measured data indicates that the FMD description gives a good insight into the structure of ^{12}C.

Table 1. Radii and transitions in ^{12}C, data: [6, 14, 15]

Energies [MeV]	Exp	FMD
$E(0_1^+)$	-92.16	-92.64
$E^*(2_1^+)$	4.44	5.31
$E(3\alpha)$	-84.89	-83.59
$E(0_2^+) - E(3\alpha)$	0.38	0.43
$E(2_2^+) - E(3\alpha)$	2.76(11)	2.77
Radii [fm]	**Exp**	**FMD**
$r_{\rm charge}(0_1^+)$	2.47(2)	2.53
$r(0_1^+)$		2.39
$r(2_1^+)$		2.50
$r(0_2^+)$ Hoyle state		**3.38**
$r(2_2^+)$ Hoyle like		**4.43**
Transitions [fm^2] or [e^{2}fm^4]	**Exp**	**FMD**
$M(E0, 0_1^+ \to 0_2^+)$	5.4(2)	6.53
$B(E2, 2_1^+ \to 0_1^+)$	7.6(4)	8.69
$B(E2, 2_1^+ \to 0_2^+)$	2.6(4)	3.83
$B(E2, 2_2^+ \to 0_1^+)$	0.73(13)	0.46

Ab initio nuclear lattice calculations [7, 8] seem to support this structure but due to the large lattice constant the angles and sites of the three-α triangles can assume only discrete values in the sampled configurations. For example the typical distance between the α-clusters in the Hoyle state is 2 to 3 lattice spacings. It will be very interesting to see if future more refined calculations on the nuclear lattice will confirm further the FMD results on the numerous aspects of the ^{12}C structure.

3 Neon isotopes and two-proton halo

The charge radii of the neon isotopes, which have been measured in Ref. [16], do not show the usual monotonic increase with mass number, while the matter radii seem to increase monotonically from ^{18}Ne on, see Fig. 3. The FMD model explains this by substantial changes in the ground-state structure. It attributes the large charge radius of ^{17}Ne to an extended two-proton halo, as seen in Fig. 4, with an s^2 component of about 40%. The leading intrinsic state (upper part of Fig. 4) has a far out reaching part consisting of two correlated protons, while the neutron distribution is almost spherical and only weakly polarized by the outer protons. This is in accord with the simplest picture that ^{17}Ne consists of an ^{15}O core plus two protons in either s^2 or d^2 configurations. Interaction cross sections [18] and longitudinal momentum distributions [19] support the halo picture. In ^{18}Ne the situation is similar but in the same simple picture the core is now the doubly magic ^{16}O, which leads to a significantly smaller s^2 component and hence a smaller charge radius.

The subsequent increase in charge radius for ^{19}Ne is of different origin. The fact that the experimental $1/2^+$ and $1/2^-$ states are almost degenerate and the cluster thresholds are pretty low, hints already at possible admixtures of states with cluster structures. Therefore it is not surprising that ^{16}O - ^{3}He and ^{15}O - ^{4}He cluster configurations admix in the tail of the wave function.

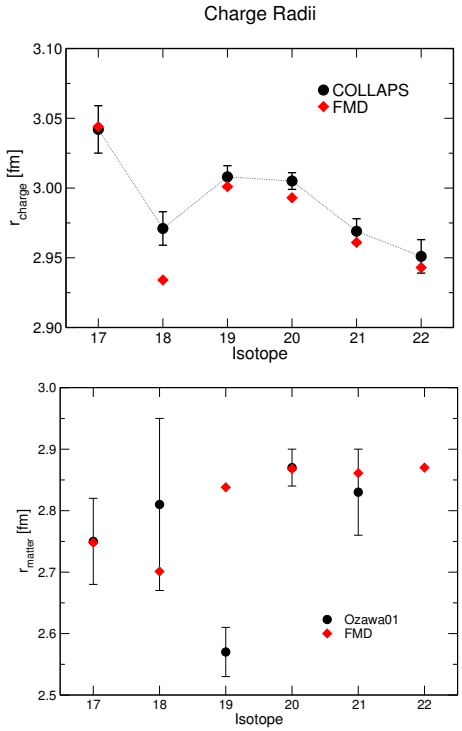

Figure 3. Top: charge radii of Ne isotopes measured by COLLAPS and calculated with FMD [16] Bottom: point mass radii, data from [17]

This admixture of cluster configurations is still very strong in ^{20}Ne but becomes smaller for heavier Ne isotopes explaining the dropping charge radii.

4 Radiative capture reaction ^{3}He$(\alpha,\gamma)^7$Be

Another application of the FMD approach is the calculation of the ^{3}He$(\alpha,\gamma)^7$Be radiative capture reaction [26]. As this reaction plays an important role in the solar proton-proton chains and determines the production of ^{7}Be and ^{8}B neutrinos [27, 28], it has been studied extensively from the experimental side in recent years [20–24]. However, it is still not possible to reach the low energies relevant for solar burning in experiment. From the theory side this reaction has been investigated using simple potential models, where ^{3}He and ^{4}He are treated as point-like particles interacting via an effective nucleus-nucleus potential, e.g., [29] or microscopic cluster models, e.g., [30, 31] where the ^{7}Be bound and scattering states are constructed from microscopic ^{3}He and ^{4}He clusters interacting via an effective nucleon-nucleon interaction. *Ab-initio* calculations using variational Monte Carlo [32] and no-core shell model wave functions [33] were used to calculate asymptotic normalization coefficients for the bound states but relied on potential models for the scattering phase shifts.

In the FMD calculation we divided the many-body Hilbert space into an external region, where the scatter-

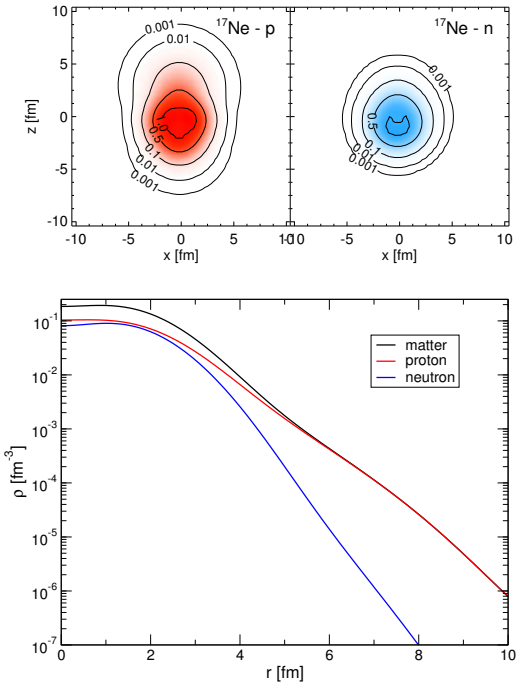

Figure 4. Top: proton and neutron density of leading intrinsic FMD state contributing to ground state of ^{17}Ne, bottom: charge distribution calculated with FMD eigenstate showing a two-proton halo [16].

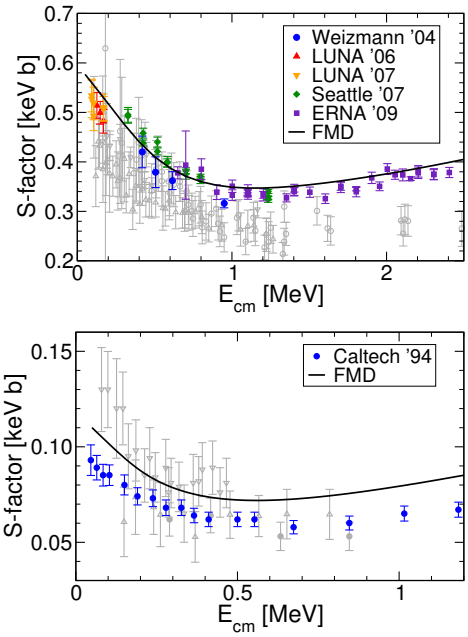

Figure 5. S-factor for capture reaction - top: ^{3}He(α,γ)^{7}Be, recent data [20–24] colored symbols, older data gray symbols - bottom: ^{3}H(α,γ)^{7}Li, recent data [25] colored, older data gray symbols.

ing states are antisymmetrized products of ^{3}He and ^{4}He clusters in their FMD ground states at various distances, and an interaction region, where FMD configurations were obtained by variation after projection on spin-parity $1/2^+$, $3/2^+$, $5/2^+$ and $3/2^-$, $1/2^-$, $7/2^-$, $5/2^-$. A constraint on the radius of the intrinsic states was used to vary the distance between the clusters. Using the microscopic R-matrix method [34] boundary conditions for bound and scattering states were implemented by matching to Whittaker and Coulomb functions at the channel radius (a = 12 fm).

The capture cross section was calculated from electromagnetic transition rates between the microscopic many-body scattering and bound states. The result for the total cross section for the ^{3}He(α,γ)^{7}Be capture is shown in form of the astrophysical S-factor in the upper part of Fig. 5. It agrees very well with the recent experimental data, both in absolute normalization and in the energy dependence. The results for the isospin mirror reaction ^{3}H(α,γ)^{7}Li is shown in the lower part of Fig. 5. Whereas the energy dependence of the calculated S-factor agrees well with the data, the absolute cross section is larger then the data by Brune *et al.* by about 15%. This is surprising as the FMD results for the ^{7}Li bound states and the scattering phase shifts are of similar quality as those for ^{7}Be.

References

[1] R.B. Wiringa, V.G.J. Stoks, R. Schiavilla, Phys. Rev. C **51**, 38 (1995)

[2] H. Feldmeier, T. Neff, R. Roth, J. Schnack, Nucl. Phys. **A632**, 61 (1998)

[3] T. Neff, H. Feldmeier, Nucl. Phys. **A713**, 311 (2003)

[4] R. Roth, T. Neff, H. Feldmeier, Prog. Part. Nucl. Phys. **65**, 50 (2010)

[5] M. Freer, et al., Phys. Rev. C **86**, 034320 (2012)

[6] W.R. Zimmermann, M.W. Ahmed, B. Bromberger, S.C. Stave, A. Breskin, V. Dangendorf, T. Delbar, M. Gai, S.S. Henshaw, J.M. Mueller et al., Phys. Ref. Lett. **110**, 152502 (2013)

[7] E. Epelbaum, H. Krebs, D. Lee, U.G. Meißner, Phys. Rev. Lett. **106**, 192501 (2011)

[8] E. Epelbaum, H. Krebs, T.A. Lähde, D. Lee, U.G. Meißner, Phys. Rev. Lett. **109**, 252501 (2012)

[9] T. Neff, J. Phys.: Conf. Ser. **403**, 012028 (2012)

[10] M. Chernykh, H. Feldmeier, T. Neff, P. von Neumann-Cosel, A. Richter, Phys. Rev. Lett. **98**, 032501 (2007)

[11] M. Chernykh, H. Feldmeier, T. Neff, P. von Neumann-Cosel, A. Richter, Phys. Rev. Lett. **105**, 022501 (2010)

[12] M. Kamimura, Nucl. Phys. **A351**, 456 (1981)

[13] Y. Funaki, A. Tohsaki, H. Horiuchi, P. Schuck, G. Röpke, Phys. Rev. C **67**, 051306(R) (2003)

[14] F. Ajzenberg-Selove, Nucl. Phys. **A506**, 1 (1990)

[15] M. Itoh, H. Akimune, M. Fujiwara, U. Garg, H. Hashimoto, T. Kawabata, K. Kawase, S. Kishi, T. Murakami, K. Nakanishi et al., Nucl. Phys. **A738**, 268 (2004)

[16] W. Geithner, T. Neff, G. Audi, K. Blaum, P. Delahaye, H. Feldmeier, S. George, C. Guénaut, F. Her-

furth, A. Herlert et al., Phys. Rev. Lett. **101**, 252502 (2008)
[17] A. Ozawa, T. Suzuki, I. Tanihata, Nucl. Phys. **A693**, 32 (2001)
[18] A. Ozawa, T. Kobayashi, H. Sato, D. Hirata, I. Tanihata, O. Yamakawa, K. Omata, K. Sugimoto, D. Olson, W. Christie et al., Phys. Lett. **B334**, 18 (1994)
[19] R. Kanungo, M. Chiba, B. Abu-Ibrahim, S. Adhikari, D.Q. Fang, N. Iwasa, K. Kimura, K. Maeda, S. Nishimura, T. Ohnishi et al., Eur. Phys. J. A **25**, 327 (2005)
[20] B.S. Nara Singh, M. Hass, Y. Nir-El, G. Haquin, Phys. Rev. Lett. **93**, 262503 (2004)
[21] D. Bemmerer et al., Phys. Rev. Lett. **97**, 122502 (2006)
[22] F. Confortola et al., Phys. Rev. C **75**, 065803 (2007)
[23] T.A.D. Brown et al., Phys. Rev. C **76**, 055801 (2007)
[24] A. Di Leva et al., Phys. Rev. Lett. **102**, 232502 (2009)
[25] C.R. Brune, R.W. Kavanagh, C. Rolfs, Phys. Rev. C **50**, 2205 (1994)
[26] T. Neff, Phys. Rev. Lett. **106**, 042502 (2011)
[27] E.G. Adelberger et al., Rev. Mod. Phys. **70**, 1265 (1998)
[28] E.G. Adelberger et al., Rev. Mod. Phys. **83**, 195 (2011)
[29] B.T. Kim, T. Izumoto, K. Nagatani, Phys. Rev. C **23**, 33 (1981)
[30] K. Langanke, Nucl. Phys. **A457**, 351 (1986)
[31] T. Kajino, Nucl. Phys. **A460**, 559 (1986)
[32] K.M. Nollett, Phys. Rev. **C63**, 054002 (2001)
[33] P. Navrátil, V.G. Gueorguiev, J.P. Vary, W.E. Ormand, A. Nogga, Phys. Rev. Lett. **99**, 042501 (2007)
[34] P. Descouvemont, D. Baye, Rep. Prog. Phys. **73**, 036301 (2010)